ARTICLE

Inactivation of IL11 Signaling Causes Craniosynostosis, Delayed Tooth Eruption, and Supernumerary Teeth

Pekka Nieminen,[1,*] Neil V. Morgan,[2] Aimée L. Fenwick,[3] Satu Parmanen,[1] Lotta Veistinen,[1] Marja L. Mikkola,[4] Peter J. van der Spek,[5] Andrew Giraud,[6] Louise Judd,[6] Sirpa Arte,[1,7] Louise A. Brueton,[2,8] Steven A. Wall,[9] Irene M.J. Mathijssen,[10] Eamonn R. Maher,[2,8] Andrew O.M. Wilkie,[3,9] Sven Kreiborg,[11,12] and Irma Thesleff[4]

Craniosynostosis and supernumerary teeth most often occur as isolated developmental anomalies, but they are also separately manifested in several malformation syndromes. Here, we describe a human syndrome featuring craniosynostosis, maxillary hypoplasia, delayed tooth eruption, and supernumerary teeth. We performed homozygosity mapping in three unrelated consanguineous Pakistani families and localized the syndrome to a region in chromosome 9. Mutational analysis of candidate genes in the region revealed that all affected children harbored homozygous missense mutations (c.662C>G [p.Pro221Arg], c.734C>G [p.Ser245Cys], or c.886C>T [p.Arg296Trp]) in *IL11RA* (encoding interleukin 11 receptor, alpha) on chromosome 9p13.3. In addition, a homozygous nonsense mutation, c.475C>T (p.Gln159X), and a homozygous duplication, c.916_924dup (p.Thr306_Ser308dup), were observed in two north European families. In cell-transfection experiments, the p.Arg296Trp mutation rendered the receptor unable to mediate the IL11 signal, indicating that the mutation causes loss of *IL11RA* function. We also observed disturbed cranial growth and suture activity in the *Il11ra* null mutant mice, in which reduced size and remodeling of limb bones has been previously described. We conclude that IL11 signaling is essential for the normal development of craniofacial bones and teeth and that its function is to restrict suture fusion and tooth number. The results open up the possibility of modulation of IL11 signaling for the treatment of craniosynostosis.

Introduction

The development of craniofacial bones and teeth involves complex tissue interactions, cell migration, and coordinated growth.[1–3] The genetic networks and signaling pathways underlying these developmental processes have been uncovered by the identification of gene mutations that cause human malformations and by mutational and experimental studies in model animals.[1,2,4] Genetic craniofacial malformations range from minor variations in tooth number to bone-formation defects such as craniosynostosis and severe malformation syndromes that affect multiple tissues and organs. Craniosynostosis, the premature closure of cranial sutures, occurs in one of 2500 newborns,[2] and although it is sometimes associated with other congenital defects, most cases of craniosynostosis appear as isolated traits. Abnormalities in tooth number constitute the most common craniofacial anomalies; the prevalence of developmentally missing teeth is 6%–8% (excluding missing third molars), and that of supernumerary teeth is 1.5%–3.5%.[4–6]

Unlike most bones in the trunk and limbs, the facial and calvarial bones develop by direct intramembranous ossification of the mesenchymal condensations without a prior cartilaginous template.[1] The cells in the center of the condensations undergo osteoblast differentiation and start deposition of the mineralizing bone matrix. The bone grows as a result of continued proliferation and differentiation of the peripheral cells. As the individual bones approach each other, fibrous sutures form between the bones and function as joints, allowing further growth of the skull and face. Growth of intramembranous bones is also characterized by bone remodeling with localized apposition and resorption by osteoblasts and osteoclasts, respectively. The flat calvarial bones grow by bone apposition at the exocranial side and at the osteogenic fronts at the sutures. Bone formation continues in the sutures until they become obliterated and the fusions between adjacent bones fix their relative positions. The calvarial and facial sutures remain patent after birth, and the timing of suture fusion is strictly regulated and varies between the individual sutures.

[1]Institute of Dentistry, Biomedicum, P.O. Box 63, University of Helsinki, FIN-00014 Helsinki, Finland; [2]Centre for Rare Diseases and Personalised Medicine, School of Clinical Experimental Medicine, College of Medical and Dental Sciences, University of Birmingham, Edgbaston, Birmingham B15 2TT, UK; [3]Weatherall Institute of Molecular Medicine, University of Oxford, John Radcliffe Hospital, Headington, Oxford OX3 9DS, UK; [4]Institute of Biotechnology, P.O. Box 56, University of Helsinki, FIN-00014 Helsinki, Finland; [5]Erasmus MC Department of Bioinformatics (Ee1540), P.O. Box 2040, 3000CA Rotterdam, The Netherlands; [6]Murdoch Children's Research Institute, Royal Children's Hospital, Flemington Road, Parkville 3052, Australia; [7]Department of Oral and Maxillofacial Diseases, P.O. Box 263, Helsinki University Central Hospital, FIN-00029 Helsinki, Finland; [8]West Midlands Region Genetics Sevice, Clinical Genetics Unit, Birmingham Women's Hospital, Edgbaston, Birmingham B15 2TG, UK; [9]Oxford Craniofacial Unit, Oxford Radcliffe Hospitals NHS Trust, John Radcliffe Hospital, Headington, Oxford OX3 9DU, UK; [10]Erasmus MC Department of Plastic Surgery (HS509) P.O. Box 2040, 3000CA, Rotterdam, The Netherlands; [11]Department of Pediatric Dentistry and Clinical Genetics, School of Dentistry, University of Copenhagen, 20 Noerre Allé, DK-2200 Copenhagen N, Denmark; [12]Department of Clinical Genetics, Copenhagen University Hospital, DK-2100 Copenhagen, Denmark
*Correspondence: pekka.nieminen@helsinki.fi
DOI 10.1016/j.ajhg.2011.05.024.

Sutural closure depends on the coordinated regulation of the proliferation, differentiation, and activity of the osteoblast precursors at the osteogenic fronts and sutures. The regulation of bone resorption at the sutures is also important, and active osteoclasts have been localized in the growing calvarial bones in mice, especially in the vicinity of the sutures and on the endocranial surface.[7] The morphogenesis of teeth occurs independently of bone, and the growing tooth germs regulate the remodeling of the surrounding jaw bone. Bone resorption around the forming teeth is necessary to allow the growth of the tooth germs and the eruption of teeth into the oral cavity.[8,9]

In craniosynostosis, some or several of the sutures between cranial and facial bones are obliterated prematurely, often prenatally. The precocious fusion of calvarial bones limits the space available for the brain growth and the skull becomes deformed as a result of compensatory growth in other sutures. Synostosis of the sutures of the maxillary complex is most often seen in syndromic forms of craniosynostosis and has been shown to lead to maxillary hypoplasia as seen in e.g., Crouzon syndrome (MIM 123500).[10] Mutations in multiple genes have been identified, most in syndromic forms of craniosynostosis, including activating mutations of fibroblast growth factor receptors (FGFRs) and loss-of-function mutations in *TWIST1* (MIM 601622), *EFNB1* (ephrin-B1 [MIM 300035]), and *EFNA4* (ephrin-A4 [MIM 601380]).[11] Involvement of other major signaling pathways, including hedgehog, is also evident.[11] At the cellular level, the mutations affect the border recognition between neural crest- and mesoderm-derived mesenchymal cells or lead to accelerated proliferation of the osteoblast precursors or to their premature differentiation into osteoblasts.[1]

Supernumerary tooth formation typically involves only one or a few extra teeth, most commonly a central incisor located in the maxillary midline, a mesiodens.[6] The occurrence of multiple supernumerary teeth is rare and is usually associated with syndromes. The molecular background of supernumerary teeth has been revealed in a few syndromes. Adenomatous polyposis coli (MIM 175100), a hereditary polypotic cancer syndrome caused by mutations in *APC* (MIM 611731), is sometimes associated with one or more supernumerary teeth or tumor-like odontomas containing numerous small teeth.[12] The *APC* gene product normally antagonizes canonical Wnt signal transduction by β-catenin. The capacity of excess β-catenin to induce de novo tooth formation has also been shown in mice.[13,14] Cleidocranial dysplasia (MIM 119600) is a syndrome caused by haploinsufficiency of transcription factor encoded by *RUNX2* (MIM 600211)[15,16] and features multiple supernumerary teeth and delayed or inhibited eruption of permanent teeth. *RUNX2* is required for bone formation, and its mutations lead to deficient bone formation and a calvarial phenotype that is opposite to craniosynostosis and features wide cranial sutures and open fontanelles.[16]

In this report, we describe the genetic mapping and identification of *IL11RA* (MIM 600939) mutations in an autosomal-recessive form of craniosynostosis associated with delayed tooth eruption, maxillary hypoplasia, supernumerary teeth, and digit abnormalities.

Subjects and Methods

Subjects

The parents of families 1–3 originated from Pakistan, and in each family the parents were first cousins. Families 4 and 5 were of north European origin and were without known consanguinity. The four affected siblings of family 1 were patients of the School of Dentistry, University of Copenhagen, Denmark. The disease in this family was called as Kreiborg-Pakistani syndrome by M. Michael Cohen Jr.[17] Family 2 consisted of two branches with a total of five affected individuals, who were ascertained at the West Midlands Regional Genetics Service, Birmingham, UK. The probands in families 3 and 4 were included in a cohort of 240 unrelated patients with syndromic or nonsyndromic craniosynostosis (Oxford cohort). The children in family 5 were patients of Sophia Children's Hospital, Erasmus MC, The Netherlands. Patients in families 2 and 5 and in the 240-patient cohort had been found to be negative for all relevant genetic testing, including testing of *FGFR1* exon 7 (MIM 136350); *FGFR2* exons 3, 5, 8, 10, 11, 14, 15, 16, and 17 (MIM 176943); *FGFR3* exons 7 and 10 (MIM 134934); and *TWIST1* exon 1 (MIM 601622). The patients and their family members were investigated clinically and radiographically. Panoramic tomograms for diagnoses of the dental phenotypes were available for families 1, 3, and 4. Peripheral-blood samples were obtained from all family members, and genomic DNA was isolated via standard methods. All studies were performed with informed consent of the participants and under permission of the local institutional ethical committees.

Genetic Mapping

For family 1, initial candidate-gene exclusion and fine mapping was performed by amplification of microsatellite markers (Dynazyme II DNA polymerase, Finnzymes, Espoo, Finland and appropriate annealing temperatures and cycle number; 55°C–59°C and 30–35 cycles, respectively), and fluorescent detection was performed in the Molecular Medicine Sequencing Laboratory, Biomedicum Helsinki. The genome-wide scan was performed at deCODE, Iceland, with 1113 markers and an average map density of 3.3 cM. Linkage mapping in families 2 and 3 was undertaken in Birmingham, UK, with the use of genome-wide SNP genotyping with the Affymetrix Human SNP 5.0 microarray and polymorphic microsatellite markers. For evaluation of linkage, Simwalk software[18] was used. The human genome build hg18 (NCBI36) was used for the marker locations, which were subsequently verified from build HG19 (GRCh37).

Mutational Analysis

For mutational analysis, exons and flanking intronic regions of candidate genes were amplified by PCR with Dynazyme Ext DNA polymerase (Finnzymes) and the use of suitable annealing temperatures and cycle number (55°C–59°C and 30–35 cycles, respectively). The PCR products were purified from free dNTPs and primers with the ExoSAP-it reagent (USB, Cleveland, OH, USA) and used as templates in sequencing with the ABI BigDye

Sequencing Kit version 3.1 (Applied Biosystems, Foster City, CA; for the primers and cycling conditions, see Table S1 available online). The sequencing products were analyzed in the Molecular Medicine Sequencing Laboratory, Biomedicum, Helsinki. The results were compared with genomic and cDNA DNA sequences from GenBank (*IL11RA*: NT_008413.17 and NM_004512.3) with bl2exe software.

Whole-genome diploid sequencing in family 5 was performed by Complete Genomics (Mountain View, CA, USA) as described before.[19] A homozygous recessive disease model was tested on the father, mother, and two affected children.

Bioinformatics

For selection of chromosome 9 candidate genes for mutational analysis, known interactions with genetic networks important in skeletal or dental development was studied in the String database and expression patterns in the GenePaint database. For alignments of the *IL11RA* sequence with other known sequences, we used BLAST searches and Clustalw. Significance of the observed changes was estimated with available software, including SIFT, PolyPhen, SNPs3D, ELM, and NetCGlyc.

IL11RA Expression Constructs

To study the effect of the *IL11RA* mutation on the receptor function, we inserted the c.886C>T mutation into the human *IL11RA* cDNA (corresponding to the GenBank reference sequence NM_004512.3; kindly provided by Tracy Willson and Lorraine Robb, Walter and Eliza Hall Institute of Medical Research, Parkville, Australia) as template by the overlap extension method.[20] Both wild-type and mutant *IL11RA* (*IL11RA/886T*) open reading frames were cloned into pEF1/Myc-His vector (Invitrogen) according to standard molecular biology techniques, and resulting plasmids were verified by sequencing.

Cell Culture and IL11 Stimulation Assays

Human 293T cells originating from embryonic kidney were maintained in Dulbecco's modified Eagle's medium (DMEM, Sigma) supplemented with 10% fetal calf serum, 2 mM glutamine, 100 U/ml penicillin, and 100 μg/ml streptomycin, and HeLa cells (of cervical cancer origin) were maintained in Minimum Essential Medium (MEM, Sigma) with the same supplements. One day prior to transfection, 500,000 cells were seeded in 6-well plates. Cells were transfected with 1 μg of pEF1-*IL11RA*, pEF1-*IL11RA/886T*, or the empty vector with the use of Fugene 6 according to the instructions of the manufacturer (Roche Diagnostics GmbH). Twenty-four hours later, cells were starved overnight in serum-free MEM medium, 0.2% bovine serum albumin (Sigma), 20 mM HEPES at pH 7.2, 50 U/ml penicillin, and 100 μg/ml streptomycin. The following day, medium was removed, and cells were stimulated for the indicated times with 100 ng/ml of IL11 (Cell Signaling Technology) in fresh serum-free medium and washed once with PBS, followed by immediate lysis in Laemmli sample buffer. Proteins were resolved by 10% SDS-PAGE and transferred onto a Hybond-C-extra membrane (Amersham), and blots were developed with the use of enhanced chemiluminesence (SuperSignal West Pico, Thermo Scientific). Two identical gels were run. In the first, phosphorylation of STAT3 was analyzed with pY705-STAT3 antibody (Cell Signaling Technology, 9145, 1:2000) with the use of horse radish peroxidase (HRP)-conjugated anti-rabbit antibody (Jackson Laboratories, 1:5000) as the secondary antibody. After blotting, the filter was quenched with 3% H_2O_2 and 0.02% sodium azide in PBS for 30 min at room temperature, and it was subsequently blotted with a primary antibody against unphosphorylated STAT3 (Cell Signaling Technology, 9139, 1:2000) followed by HRP-conjugated anti-mouse secondary antibody (Jackson Laboratories, 1:5000). For verification of the protein levels of the wild-type and mutant IL11RA, the second gel was blotted either with an anti-c-*myc* antibody (Roche Diagnostics GmbH, 11 667 149 001), according to manufacturer's instructions, which was followed by HRP-conjugated anti-mouse antibody, or with IL11RA antibody (R&D Systems, MAB1977, 1:1000) and HRP-conjugated anti-mouse secondary antibody.

In Situ Hybridization

Heads of staged embryos and postnatal mice of the NMRI strain were fixed in 4% paraformaldehyde, embedded in paraffin, and serially sectioned at 7 μm. The expression analysis by in situ hybridization was carried out according to standard protocols with the use of ^{35}S-UTP labeling (Amersham). Mouse *Il11ra* probe was cloned from E14 mouse mandibular cDNA into a pCRII-TOPO vector (Invitrogen). The probe included the nucleotides 475–1294 of the *Il11ra* open reading frame (NM_010549.2). The *bone sialoprotein* (*Bsp*) probe was a kind gift from Marian Young, NIDCR, NIH.

Analysis of Mouse Mutants

The generation of the *Il11ra* null mutant mice has been described previously.[21] The mice were maintained on a C57BL/6 background, genotyped by multiplex PCR, and housed in an SPF facility in microisolater vented cages. Ethical approval was obtained from Murdoch Children's Research Institute (A583). Heads of 6-week-old *Il11ra* null mutant homozygote and heterozygote mice and wild-type littermates were fixed for 3 days in 95% ethanol. Skeletal preparations were made by boiling the heads for 30 min and removing the soft tissues. The microCT analysis was performed at a 10 μm resolution with the use of a SkyScan 1172 instrument in the BioMater Centre at the University of Kuopio, Finland.

Results

Craniofacial and Dental Findings

Four of the six children in family 1 were affected, whereas two daughters (IV:1 and IV:5) and the parents had normal craniofacial features (Figure 1). The parents and healthy siblings had normal head circumference and jaw relationships and had no history or signs of supernumerary teeth formation or delayed tooth eruption (Table 1). The oldest affected child (IV:2) was a girl who was referred at the age of 11.4 years by an orthodontist because of maxillary hypoplasia with class III malocclusion and abnormal tooth eruption. The skull radiographs revealed premature fusion of all calvarial sutures, increased digital markings, and a reduced cranial base angle. The other three affected children were first investigated at comparable ages (IV:3 at 10.8 years, IV:4 at 8.3 years, and IV:6 at 10.6 years). The two affected boys (IV:3 and IV:4) had complex synostosis of all calvarial sutures. Individual IV:3 underwent surgery for coronal synostosis at 4 years of age and had a high, steep forehead and a reduced cranial base angle.

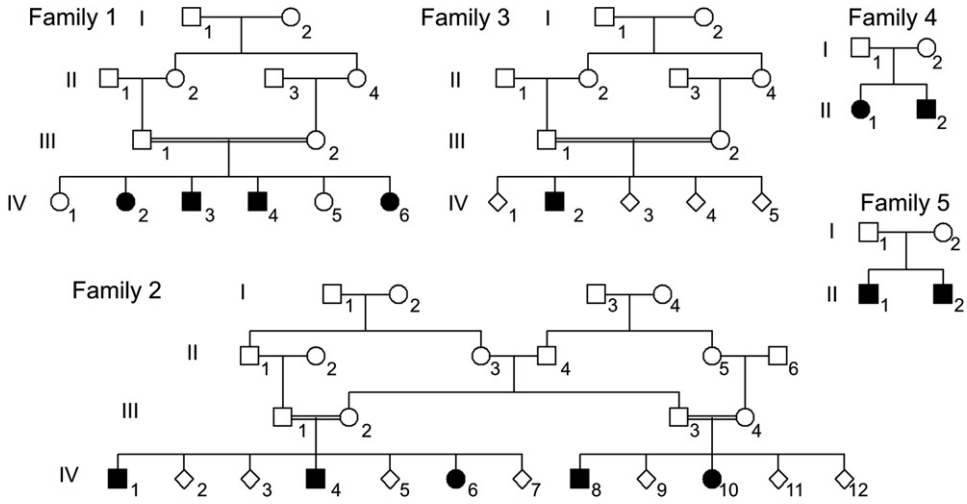

Figure 1. Pedigrees of the Families
Families 1, 2, and 3 were used in the genetic mapping. Squares, females; circles, males; diamonds, sex not indicated; filled, affected; open, unaffected, double line connecting parents, consanguinity.

Individual IV:4 had a strikingly reduced head length and a brachycephalic and oxycephalic head shape with increased height and a flattened cranial base (Figure 2A). The youngest girl (IV:6) had fused sagittal and coronal sutures but patent lambdoid sutures, resulting in a dolichocephalic skull with a protruding forehead and an increased cranial base angle (Figure 2B). All four affected children had some degree of midfacial hypoplasia associated with class III malocclusion. Their permanent teeth had all developed, but the eruption, especially of canines and premolars, was delayed and several teeth erupted ectopically. They all also had supernumerary teeth, from 1 to 7 in number (Tables 1 and 2, Figures 2C and 2D), observed in the incisor, canine, and premolar regions. These teeth were delayed for approximately 4 years in their formation as compared to their counterparts in the permanent dentition, and they were located lingually and occlusally to the normal permanent teeth.

In family 2, a total of five children with craniosynostosis had been born to two consanguineous and closely related couples (Figure 1). The craniosynostosis was diagnosed in individual IV:1 at the age of 2 years because of severe proptosis and papilloedema (Table 1). Multiple suture synostosis was confirmed radiologically. Four other younger children in the family were subsequently diagnosed (IV:4, IV:6, IV:8, and IV:10), and all were surgically treated with combined craniofacial correction or bicoronal craniectomy. Upon examination after surgery, IV:1 was noted to have midface hypoplasia, proptosis, a beaked nose, and brachycephaly; the other affected children had more subtle clinical findings, with a flat or sloping forehead, a reduced occipito-frontal circumference (OFC), and mild proptosis. All affected children had broad great toes with valgus deformities. Other variable clinical features included mild syndactyly of the fingers and toes, clinodactyly, prominent helical crura, large upper lateral incisors, high palate, and short stature (Table 1). Although one of the children had a Crouzon-like facies, the family was not considered typical of any of the previously described craniosynostosis syndromes.

The only affected individual in family 3, a male (IV:2, Figure 1), was the second of five siblings. There was no family history of unusual skull shapes or dental problems. He presented at the age of 13 months after being noted during a routine health check as having an unusually shaped head (Figures 2E and 2F; Table 2). He had had a high pointed forehead with prominent midline ridging, and the dura was palpable and bulged through holes that were eroding the skull posteriorly. There was slight exorbitism and bilateral papilloedema. The remainder of the examination, including hands and feet, was normal, and development was appropriate for age. A plain radiograph of the skull showed marker copper beating, and a computed tomogram showed a trigonocephalic deformity consistent with metopic synostosis, and closure of the sagittal, coronal, and lambdoid sutures. He underwent fronto-orbital advancement and remodeling with lateral panel extension at the age of 2.0 years. At the age of 5.2 years, he underwent calvarial expansion by forehead advancement because of the recurrence of raised intracranial pressure. By the age of 12 years, he was noted to have a compacted palate with dental disarray and persisting deciduous teeth, and he underwent orthodontic assessment. He had evidence of maxillary hypoplasia with class III malocclusion; all permanent teeth were present, with palatal eruption of right maxillary premolars and ectopic eruption of maxillary third molars.

The female proband in family 4 (II:1, Figure 1) was the first of two siblings born to unrelated parents of white north European origin. An unusual head shape was noted at birth. At the age of 13 years, a skull radiograph, obtained because of dental problems, demonstrated total vault

Table 1. Phenotypic Description of the Affected Family Members in Families 1 and 2

	Family 1				Family 2			
Patient	IV:2	IV:3	IV:4	IV:6	IV:1	IV:4	IV:8	IV:10
Sex	female	male	male	female	male	male	male	female
First examination	11.4 yr	10.8 yr	8.3 yr	10.6 yr	9 yr	3 yr	8 yr	2 yr
Papilloedema	mild	mild		mild	severe	mild	mild	mild
Neurodevelopment	normal	normal	normal	normal	learning difficulties	normal	normal	normal
Increased digital markings or copper beating	yes	yes	yes	yes				
Metopic synostosis	yes	yes	yes	yes	yes	yes	yes	yes
Coronal synostosis	yes	yes	yes	yes	yes	yes	yes	yes
Sagittal synostosis	yes	yes	yes	yes	yes			yes
Lambdoid synostosis	yes	yes	yes	no	no			yes
Cranial surgery	no	4 yr	no	no	2.3 yr	2.5 yr	2 yr	1.5 yr
Skull shape			brachycephaly and oxycephaly		brachycephaly	flat occiput, ridged metopic suture	brachycephaly	
Reduced OFC					3rd centile	< 3rd centile	< 3rd centile	< 3rd centile
Forehead		high, steep	backward slope	protruding	flat	sloping	flat	flat
Maxillary hypoplasia	yes (SNA 73°)	yes (SNA 76°)	yes (SNA 75°)	yes (SNA 78°)	marked	mild	mild	mild
Nose					beaked			broad, flat bridge
Cranial base	reduced angle (n-s-ba 125°)	reduced angle (n-s-ba 126.5°)	flattened (n-s-ba 141.5°)	increased angle				
Palate						high	narrow	
Constricted nasopharynx	yes	yes						
Occlusion	class III	class III	incisors edge-to-edge	incisors edge-to-edge				
Delayed tooth eruption	yes	yes	yes	yes				
Teeth	2 supernum	1 supernum	2 supernum	7 supernum		large lateral incisors	large lateral incisors	
Broad first toes, hallux valgus					yes	yes	yes	yes
Syndactyly					mild 2-3 toe		mild 2-3 toe	mild 2-3 toe
Clinodactyly					yes			
Other					Crouzon like features	short stature, prominent ears	short phalanges, dysplastic fingernails	

Empty cells indicate unreported or unknown data. Abbreviations are as follows: n-s-ba, nasion-sella-basion angle; OFC, occipito-frontal circumference; SD, standard deviation unit; SNA, sella-nasion-point A angle.

sutural fusion with copper beating (Table 2). At that time, she was noted to have mild hypertelorism with prominent eyes, a slightly beaked nose, maxillary hypoplasia, and marked turricephaly. Her visual acuity was 6/5 in the right eye and 6/12 in the left eye, and she had an enlarged blind spot in the left eye. By the age of 19 years, multiple extractions of her deciduous teeth had been required to enable eruption of the permanent teeth. Her brother was not assessed in detail but was reported to have a similar skull shape and history of dental problems.

The patients in family 5 are brothers from healthy Dutch nonconsanguineous parents (Figure 1). The oldest brother

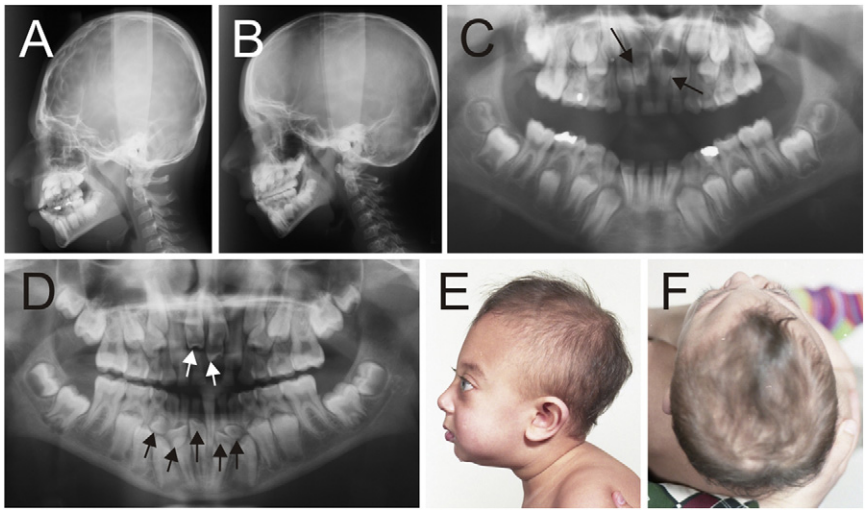

Figure 2. Craniosynostosis and Supernumerary Teeth
(A) Lateral cephalometric radiograph of IV:4 in family 1 taken at an age of 10 years, showing the oxycephalic shape of the head resulting from complex bilateral coronal craniosynostosis and maxillary hypoplasia.
(B) Lateral cephalometric radiograph of IV:6 in family 1 taken at an age of 10 years, showing the dolichocephalic shape of the head resulting from complex craniosynostosis.
(C) Panoramic tomogram of IV:4 in family 1 taken at an age of 9 years, showing two supernumerary teeth (arrows).
(D) Panoramic tomogram IV:6 in family 1 taken at an age of 10 years, showing seven supernumerary teeth (arrows).
(E) Craniofacial appearance of the affected boy IV:2 in family 3 at the age of 13 months. Note mild exorbitism in the absense of characteristic dysmorphic features.
(F) Superior view of the trigonocephalic skull of the affected boy IV:2 in family 3 at the age of 13 months.

(II:1) was first seen at the age of seven with a ridge over the sagittal suture, a bony bulge at the vertex, a flattened forehead, and hypertelorism (Table 2). Furthermore, his maxilla was hypoplastic, resulting in exorbitism and mild obstructive sleep apnea. His X-ray showed synostosis of all cranial sutures. He was diagnosed with attention deficit hyperactivity disorder and an IQ of 70–80. The younger brother (II:2) had a scaphocephalic shape of the head, with overt frontal bossing. Mild exorbitism and midface hypoplasia were observed. X-ray proved the sagittal suture to be closed. In the following years, motor development turned out to be normal, but a slight delay in speech was noted.

Genetic Mapping and Mutation Identification

After exclusion of linkage to *RUNX2,*which is known to be implicated in bone and tooth development, we performed genome-wide search in family 1, and we identified several candidate regions (chromosomes 1, 4, 8, 9, 12, and 14) in which the affected siblings shared the same homozygous genotype not present in the unaffected siblings. However, fine-mapping studies then excluded all regions except chromosome 9 in which the area of shared homozygosity extended from D9S265 in 9p21.3 (25,385,580 bp) to D9S175 in q21.13 (77,947,763 bp) (Figure S1). Multipoint linkage analysis gave a Simwalk location score of 3.26, considered as significant evidence for linkage, over the entire region (Figure 3A).

According to the human genomic sequence, the region identified in family 1 contains ≥200 RefSeq genes. Eleven of these genes were selected for mutational analysis on the basis of known function and/or expression patterns. Direct sequencing of the coding regions of these genes revealed only one previously undocumented sequence variant that was present in a homozygous state in all four affected family members but not in the unaffected members. This variant, a c.886C>T transition in exon 9 of *IL11RA*, resulted in a p.Arg296Trp substitution (Figure 3B).

For family 2, the genome-wide analysis showed that all five affected children shared a common haplotype on chromosome 9 between SNPs rs10967436 (26,608,592 bp) and rs7044969 (82,078,913 bp), overlapping with the region of homozygosity in family 1. Genotyping of parents and siblings with microsatellite markers from chromosome 9 confirmed informative linkage with a maximal location score of 4.18 (Figure 3A, Figure S2). The chromosome 9 microsatellite markers typed for family 3 showed homozygosity within the candidate regions in families 1 and 2 and a maximal location score of 1.55 (Figure S3, data not shown).

Subsequent mutational analysis of exons of *IL11RA* in samples from families 2 and 3 and from the cohort of craniosynostosis-affected individuals from Oxford revealed three other mutations that were present in a homozygous state in the affected family members (Figures 3C–3E). In the six affected individuals from families 2 and 3, homozygous C>G transversions were detected in exon 8, at positions 662 (family 2) or 734 (family 3), resulting in p.Pro221Arg and p.Ser245Cys substitutions, respectively. In another sample from the Oxford cohort (II:1 in family 4), a homozygous transition, c.475C>T in exon 6, encoding the nonsense mutation p.Gln159X, was identified. None of the unaffected siblings tested in families 2 and 3 was homozygous for these mutations. In addition, none of these sequence changes was observed in 400 control samples of Finnish, other European, or Pakistani (n = 186) origin, and they are not present in the dbSNP or 1000 Genomes databases. In addition, heterozygous nonsynonymous variants, two of which are listed in dbSNP, were found in different single individuals of the Oxford cohort

Table 2. Phenotypic Description of the Affected Family Members in Families 3–5

	Family 3	Family 4	Family 5	
Patient	IV:2	II:1	II.1	II:2
Sex	male	female	male	male
First examination	13 months	13 yr	7 yr	1 yr
Papilloedema	moderate	mild	Yes	optic atrophy
Neurodevelopment	persistent language delay, special needs education	normal	ADHD	slight speech delay
Increased digital markings or copper beating	yes	yes	yes	
Metopic synostosis	yes	yes	yes	no
Coronal synostosis	yes	yes	yes	no
Sagittal synostosis	yes	yes	yes	yes
Lambdoid synostosis	yes	yes	yes	no
Cranial surgery	2 yr, 5.2 yr	no		
Skull shape	trigonocephaly	turricephaly, hypertelorism	ridge over the sagittal suture, hypertelorism	scaphocephaly, frontal bossing
Reduced OFC	3rd centile	75 th centile (19 y)	~1SD	
Forehead	high pointed		flat	
Maxillary hypoplasia	yes	yes	yes	mild
Nose		slightly beaked		
Cranial base				
Palate	compacted	high-arched		
Constricted nasopharynx	adenotonsillectomy 8 yr		mild	
Occlusion	class III, dental crowding			
Delayed tooth eruption	yes	yes		
Teeth				
Broad first toes, hallux valgus	no	no	no	no
Syndactyly	no	no	no	no
Clinodactyly	no	no	no	no
Other		Crouzon suggested		

Empty cells indicate unreported or unknown data. Abbreviations are as follows: OFC, occipito-frontal circumference; and SD, standard deviation unit.

as follows: 128C>T (Ser43Phe; rs76429508), c.130G>A (p.Val44Met), c.193C>A (p.Pro65Thr; rs11575589), c.871G>A (p.Val291Ile), c.1090_1104delGAGCAGGTAGC TGTG (p.Glu364_Val368del).

The three missense mutations encoded within exons 8 and 9 affect amino acids that are located in the second extracellular fibronectin type domain III (FNIII) (Figure 3F). This domain of IL11RA, which provides the predominant contribution for the binding of the IL11 ligand,[22] is extremely conserved, and the three amino acids affected by the mutations are absolutely conserved in all mammalian *IL11RA* orthologs (Figure S4). Proline 221 is conserved in all vertebrates, whereas serine 245 is conservatively replaced by threonine in *Xenopus* and arginine 296 by lysine in the nonmammalian orthologs (Figure S4). Proline 221 is conserved also in the corresponding positions of two related human cytokine receptors ciliary neurotrophic factor receptor (CNTFR) and interleukin 6 receptor alpha (IL6RA), whereas serine 245 is replaced by threonine in human CNTFR and arginine 295 by lysine in CNTFR and by glutamine in IL6R. Evaluation of these amino acid positions by bioinformatic software (SIFT, PolyPhen, and SNP3d) suggests that the observed changes are damaging for the protein function (Table 3). A similar analysis suggested that two of the heterozygous changes present in the Oxford cohort as well as two SNPs reported in the dbSNP database may also affect protein function (data not shown).

After the whole-genome sequencing in family 5, a homozygous duplication, c.916_924dup, was detected in the

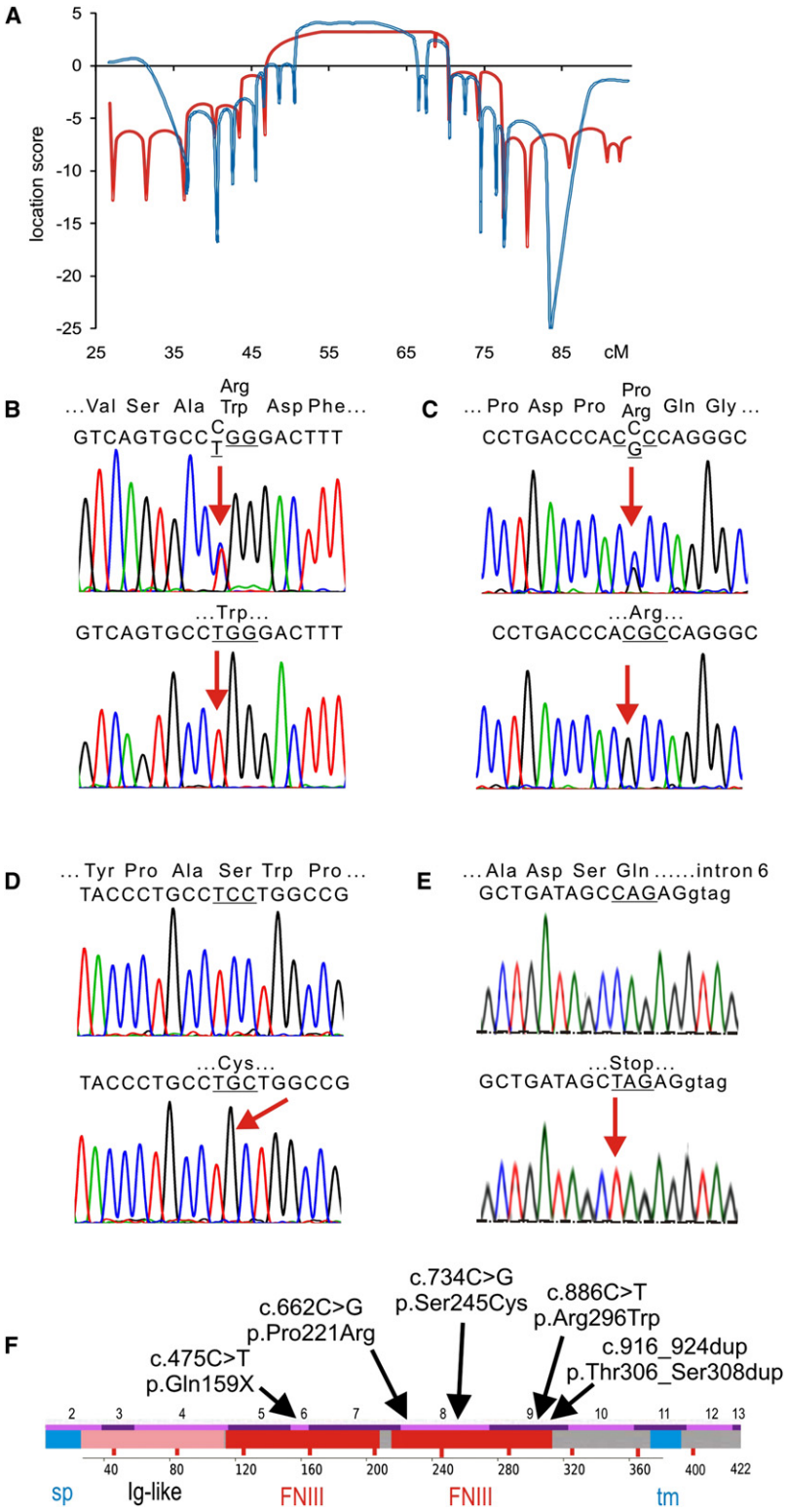

Figure 3. Genetic Mapping and Mutational Analysis

(A) Location score curves from the Simwalk multipoint analysis of chromosome 9 microsatellite marker genotypes. red, family 1; blue, family 2.

(B) Chromatograms showing the c.886C>T (p.Arg296Trp) mutation in exon 9 of *IL11RA* in family 1. Upper, unaffected heterozygous father (III:1); lower, affected homozygous son (IV:4).

(C) Chromatograms from the sequencing of exon 8 of *IL11RA* in family 2 showing the c.662C>G (p.Pro221Arg) mutation in a heterozygous carrier (upper) and homozygous state in one of the affected individuals (lower panel).

(D) Chromatograms showing the c.734C>G (p.Ser245Cys) mutation in exon 8 of *IL11RA* in family 3. Upper, unaffected control; lower, affected homozygous son (IV:2).

(E) Chromatograms from sequencings of exon 6 of *IL11RA* showing the homozygosity in the proband of family 4 (II:1) for c.475C>T (p.Gln159X; upper, unaffected control; lower, II:1 of family 4).

(F) Scheme of the IL11RA protein structure and location of the mutations. The missense mutations are all located in the second fibronectin-type domain III (FNIII). Mapping to exons is shown above and amino acid numbers below the scheme. sp, signal peptide; Ig-like, immunoglobulin-like domain; tm, transmembrane domain.

affected children and was present in a heterozygous state in the parents. This mutation was not observed in any other samples, and it is not present in the dbSNP or 1000 Genomes databases. The 9 bp duplication adds a third Thr-Trp-Ser repeat (p.Thr306_Ser308dup) and affects a conserved Trp-Ser-NNN-Trp-Ser motif of the class I cytokine receptors in the C-terminal end of the second FNIII domain (Figure 3F).[22] Bioinformatic tools (ELM and NetCGlyc) predict that the conserved motif contains a C-mannosylation signal and that the duplication strengthens this signal by adding additional C-mannosylation sites (Table 3).

The Arg296Trp Mutation Renders the IL11RA Unable to Mediate the IL11 Signal

Stimulation of IL11RA by IL11 (MIM 147681) triggers activation of the glycoprotein gp130 (MIM 600694).[23–25] As a consequence of gp130 activation by the IL11/IL11RA complex, the Janus kinase/signal transducer and activator of transcription (JAK/STAT) pathway, predominantly STAT3 (MIM 102582), is stimulated.[26,27] We studied the effect of the c.886C>T (p.Arg296Trp) mutation on IL11RA function by comparing the ability of the wild-type and mutant IL11RA to induce STAT3 phosphorylation in transfected 293T cells. The protein levels of wild-type and mutant IL11RA in transfected 293T cells were comparable (Figure 4A), and no apparent changes in their intracellular localization were observed when analyzed by indirect

Table 3. Bioinformatic Analysis of IL11RA Variants

	p.Pro221Arg	p.Ser245Cys	p.Arg296Trp	p.Thr306_Ser308dup
Mammalian conservation	yes	yes	yes	yes
Vertebrate conservation	yes	conserved in birds, Thr in *Xenopus*	Lys in nonmammals	yes
Domain	second FNIII	second FNIII	Second FNIII	extracellular
SIFT	affects protein function (0.00)	affects protein function (0.00)	affects protein function (0.00)	n.a.
PolyPhen	probably damaging	probably damaging	probably damaging	n.a.
PolyPhen PSIC score difference	2.499	1.556	2.255	
SNPs3D	harmful	harmful	harmful	n.a.
SNPs3D SVM profile	~3.26	~1.87	~1.73	
ELM	no difference	no difference	no difference	stronger mannosylation motif
NetCGlyc	no difference	no difference	no difference	additional mannosylation motifs (1–4)

Second FNIII, second fibronectin type III domain.

immunofluorescence (data not shown). Application of IL11 to nontransfected 293T cells or cells transfected with an empty control vector (pEF1/Myc-His without *IL11RA*) led to modest phosphorylation of STAT3 due to activation of endogenous IL11RA (Figure 4A and data not shown). However, IL11 induced a much stronger response in cells transfected with wild-type *IL11RA*, whereas phosphorylation of STAT3 in *IL11RA/886T*-transfected cells did not exceed the level observed in the control cells (Figure 4A). Similar data were obtained in HeLa cells, although there was a higher endogenous activity of IL11RA (Figure 4B). These results strongly suggest that the Arg296Trp mutation rendered IL11RA unable to stimulate STAT3-mediated intracellular signal transduction.

Il11ra Is Expressed in the Craniofacial and Dental Mesenchyme

The expression of the murine ortholog *Il11ra* was previously localized to mesenchymal tissues in mouse embryos, with prominent expression in the craniofacial mesenchyme and later in the dental mesenchyme of incisors.[28] We performed a more detailed expression analysis by in situ hybridization in embryonic and early postnatal mouse craniofacial tissue sections. In embryonic day 14 (E14) embryos, rather uniform expression was observed in mesenchymal tissues (data not shown). The expression in mesenchymal cells was generally increased at E17 and was particularly strong in the dental papilla of the molar and incisor tooth germs (Figures 5A and 5D). In addition, the osteogenic mesenchyme surrounding the forming mandibular, maxillary, and calvarial bones expressed *Il11ra* intensely, but the differentiated osteoblasts associated with the bone matrix were devoid of transcripts in all bones (Figures 5B and 5C and data not shown). At postnatal day 4, intense expression continued in the dental papilla mesenchyme but was downregulated in the differentiated odontoblasts (Figure 5G). Expression was strong in mesenchyme associated with cranial and facial bones, in particular in all examined sutures, including midpalatal, frontal, and sagittal sutures (Figures 5E and 5H). Expression of *Il11ra* was apparent in the mesenchyme around the osteogenic fronts of calvarial bones but was downregulated during the terminal differentiation of the osteoblasts (compare Figures 5E and 5H with Figures 5F and 5I, respectively).

Il11ra Null Mutant Mice Have a Shortened and Twisted Snout and Synostosis of the Facial Sutures

The phenotype of the *Il11ra* null mutant mouse has been analyzed previously. In addition to female infertility as a consequence of defective uterine response, abnormalities in bone remodeling were reported in the long bones;[29,30] however, the skull phenotype was not reported. We collected heads from 6-week-old mutant mice and their heterozygous and wild-type littermates. In skeletal preparations of the homozygote mutants, we observed several skulls that were abnormally short. Strikingly, in some male homozygote null mutant heads, the snouts were twisted and shorter than in heterozygous or wild-type littermates (Figures 6A and 6B). Some of the skulls were subsequently subjected to microCT scanning. We did not observe synostosis in any of the calvarial sutures. However, premaxillary sutures in the homozygous mutants showed signs of suture inactivation (Figures 6C and 6D), especially on the side where the maxilla was shortest (Figures 6E and 6F). The inactivation of sutures presumably impairs antero-posterior growth and also leads to the twisting of the snout. The teeth of the *Il11ra* null mutants appeared normal, but several mutants with shortened snouts had severe dental malocclusion, in that the upper teeth were posteriorly positioned in relation to the lower teeth (Figure 6G).

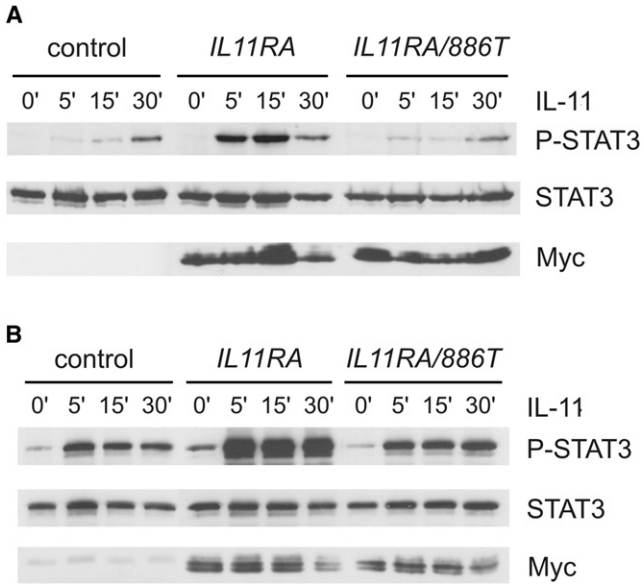

Figure 4. The p.Arg296Trp Mutation Compromises the Ability of IL11RA to Induce STAT3 Phosphorylation
293T (A) or HeLa (B) cells transfected with control vector, or with vectors expressing myc-tagged wild-type *IL11RA* or mutant *IL11RA* (*IL11RA/886T*) were stimulated for the indicated times with IL11. Levels of phosphorylated STAT3, total STAT3, and myc-tagged IL11RA were visualized by immunoblotting. In both 293T and HeLa cells transfection with wild-type *IL11RA* rendered cells much more responsive to IL11 while the level of phospho-STAT3 in *IL11RA/886T*-transfected cells was comparable to cells transfected with the control vector.

Discussion

Here, we have described a recessively inherited craniofacial syndrome and identified causative mutations in *IL11RA*. *IL11RA* encodes the interleukin receptor alpha, a well-characterized cell-surface receptor mediating interleukin-11 (IL11) signaling through activation of the coreceptor gp130. To our knowledge, neither IL11 nor gp130 signaling has previously been linked to congenital malformations in humans.

The syndrome features synostosis of calvarial bones, maxillary hypoplasia, delayed and ectopic tooth eruption, formation of supernumerary teeth, and minor digit abnormalities. Craniosynostosis was observed early in infancy and affected all calvarial sutures, resulting in variable abnormal skull shapes. The phenotypes suggest that IL11 signaling is important in all sutures and may not have a predisposing effect for synostosis of specific craniofacial suture(s). Maxillary hypoplasia is commonly associated with synostosis of the calvarial bones, particularly in severe forms of craniosynostosis such as Crouzon and Apert syndromes (MIM 123500 and 101200, respectively),[10] as a result of precocious ossification of maxillary sutures. In the affected children in this study, the severity of maxillary hypoplasia varied from moderate to mild and was less pronounced compared to severe cases of Crouzon syndrome, suggesting a later onset of fusion of sutures of the maxillary complex associated with *IL11RA* mutations.[10] The minor digit abnormalities that were reported in family 2 are common findings in several craniosynostosis syndromes, but we are not aware of earlier reports in which craniosynostosis is associated with delayed tooth eruption and extra tooth formation.

The genome-wide homozygosity-mapping studies in the three consanguineous families revealed large overlapping homozygous regions of chromosome 9 in the affected children. After the mutational analysis of plausible candidate genes in family 1, we identified a homozygous point mutation, p.Arg296Trp, in *IL11RA*. Examination of this gene in other families and a large patient cohort led to the identification of three other homozygous point mutations, p.Pro221Ser, p.Ser245Cys, and p.Gln159X, as well as of a 3 aa duplication, p.Thr306_Ser308dup. The mutations were not detected in any of the control samples, even in a heterozygous state, excluding the possibility that they are common polymorphisms and collectively providing evidence that the mutation of *IL11RA* is causative in these families.

Currently, the only known ligand for the IL11RA receptor is interleukin-11. The binding of IL11 to IL11RA (alpha receptor) leads to the formation of a hexameric cell-surface complex of two ligands, two alpha receptors, and two gp130 signaling coreceptors (beta receptors).[31] The formation of the signaling complex enables phosphorylation of the intracellular tyrosines of gp130 to trigger intracellular signal transduction, through either the JAK/STAT1/3 or the SHP2/MAPK/ERK phosphorylation cascades.[26,27] The three missense mutations described above affect conserved amino acids in the second extracellular fibronectin type III domain that is mainly responsible for the interactions of the receptor with the ligand and the coreceptor gp130.[22,32] Cell-transfection experiments indicated that the p.Arg296Trp mutation renders the receptor unable to mediate downstream phosphorylation of STAT3, suggesting that the mutation causes a loss of gene function. The nonsense mutation p.Gln159X is predicted to truncate the protein upstream of the ligand-binding second fibronectin type III domain and/or lead to nonsense mediated decay of the mRNA, supporting the conclusion that the phenotypes arise from complete loss of IL11 signal transduction.

The causative role of impaired IL11 signaling in the craniosynostosis phenotype of our patients was supported by studies of *Il11ra* null mutant mice. At 6 weeks of age, these mice phenocopied the maxillary hypoplasia and class III malocclusion in our patients. As a likely explanation, signs of inactivation of premaxillary sutures were evident, especially on the side of the curvature of the snout. The findings support the idea that the growth disturbance is late compared to that seen in Crouzon and Apert syndromes. Skewing of the snout was also observed in the mouse model for another craniosynostosis syndrome, Muenke syndrome (MIM 602849), harboring a specific missense

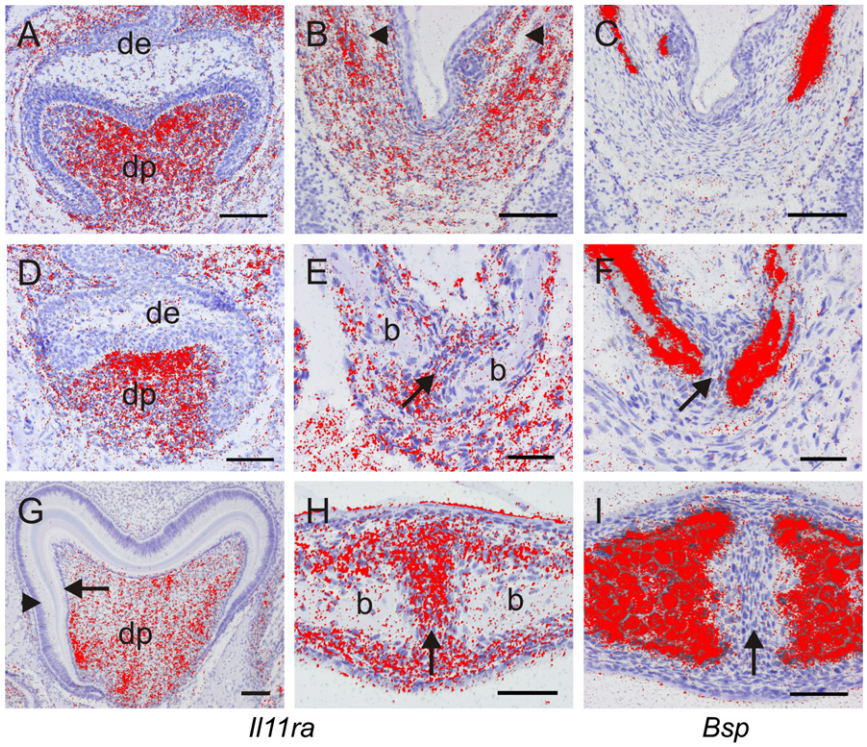

Figure 5. Expression of *Il11ra* in Developing Mouse Skull and Teeth
(A–D) In E17 embryos, *Il11ra* is expressed in the dental papilla and the surrounding mesenchyme of the bell stage first molar (A) and the cap stage second molar (D). Expression is intense in the calvarial mesenchyme of the (prospective) sagittal suture (B). The negative areas in B (arrowheads) represent differentiated osteoblasts and deposited bone matrix as shown by expression of bone sialoprotein (*Bsp*) in C. de, dental epithelium; dp, dental papilla. Scale bars represent 100 μm.
(E–I) In postnatal day 4 pups *Il11ra* is expressed (E) in calvarial mesenchyme and in the frontal suture (arrow) but excluded from areas (b) of bone matrix deposition expressing *Bsp* (F). In the first molar, deposition of the dental hard tissues is ongoing and *Il11ra* is expressed in the dental pulp (dp) (G). The expression is weaker in the coronal region of the pulp and absent from the odontoblasts (arrow) and ameloblasts (arrowhead). *Il11ra* is expressed in the mesenchyme of the secondary palate including the palatal suture (arrow) (H). The negative areas (b) represent differentiated osteoblasts and bone matrix deposition as shown by expression of *Bsp* in (I). Scale bars represent 100 μm in (G) and 50 μm in (E–I).

mutation in *Fgfr3*.[33] As in *Il11ra* mice, the phenotype was not fully penetrant and synostosis of the calvarial sutures was observed only rarely.

IL11 is widely expressed in mesenchymal and stromal cells and has been associated with a variety of biological functions, including hematopoiesis, placental decidualization, hippocampal development, and tumorigenesis.[29; 34–37] Roles for IL11 in the regulation of bone formation and remodeling have been demonstrated in several in vitro and in vivo studies.[38] Bone remodeling is a key process in the homeostasis of all bones, and it is especially important in the growth and development of the craniofacial bones that form directly from the mesenchyme without a cartilaginous template and have to adapt to the growth of the brain and to the functional needs of mastication.[39] Bone remodeling involves tight spatiotemporal control of bone apposition by the osteoblasts derived from osteogenic mesenchyme and of bone resorption by the osteoclasts of hematopoietic origin, and it is controlled by systemic and local factors and by complex crosstalk between the two cell types.[40,41]

IL11 supports the differentiation of osteoblasts from cultured bone marrow cells, mesenchymal cell lines, and periodontal ligament cells.[42–44] In adult transgenic mice, overexpression of *Il11* in bone leads to increased apposition and preservation of bone with apparently cell-autonomous activation of osteoblast differentiation.[43] IL11 acts synergistically with bone morphogenetic proteins (BMPs) in promoting bone apposition and target gene activity in osteoblastic cells in vitro and during bone repair.[43,45,46] Furthermore, because *Il11* expression is upregulated by mechanical loading in osteoblasts, it may be one of the molecular mediators of functional regulation of bone growth and remodeling.[47]

Although there is substantial evidence that IL11 signaling supports osteoblast differentiation and function, it also has a significant role in osteoclast differentiation. The previous studies on the long-bone phenotype of *Il11ra*-deficient mice indicated that blocking IL11 signaling decreases both bone formation and resorption, and the trabecular bone volume was increased while the bone dimensions and cortical bone thickness were slightly reduced.[30] Interestingly, when osteoblast or osteoclast precursors from these mice were cultured, the osteoblasts differentiated normally but osteoclast differentiation was impaired in a cell-autonomous fashion, suggesting that the primary defect resides in osteoclast differentiation.[30] This finding is in line with earlier studies showing that IL11 signaling supports osteoclast differentiation indirectly via *TNFSF11* (earlier called *RANKL*, MIM 602642) induction in osteoblasts[48–51] and also by direct TNFSF11-independent action on osteoclast precursors.[52]

In our in situ hybridization analysis of *Il11ra* expression in the forming craniofacial bones of embryonic and postnatal mice, we observed intense expression in the mesenchyme surrounding the bones while the differentiated *Bsp*-positive osteoblasts in the sutures and developing

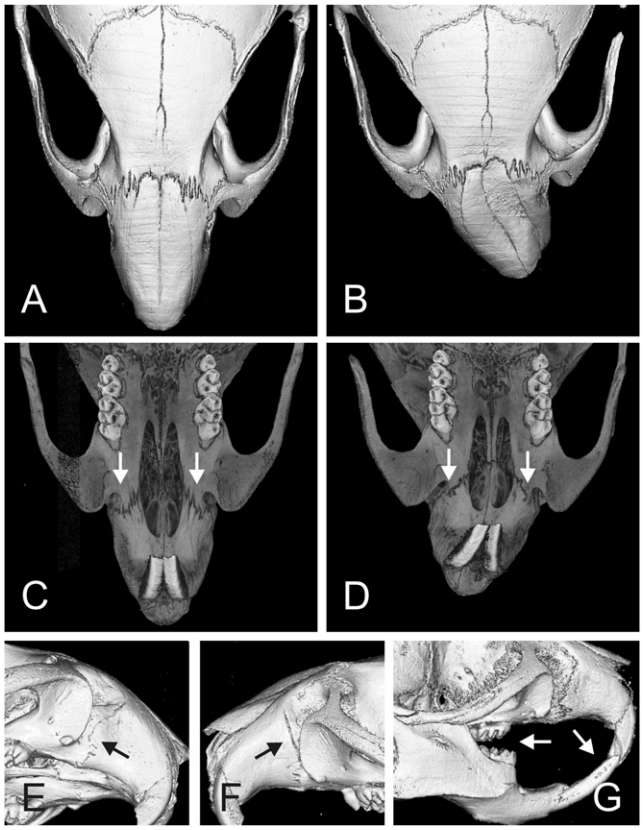

Figure 6. Craniofacial Phenotype in the *Il11ra* Null Mutant Mouse

(A and B) MicroCT image of anterior part of skull of a wild-type mouse (A) and a homozygous *Il11ra* null mutant littermate (B). The snout of the mutant mouse is significantly shorter and twisted to the left.

(C and D) Inferior view of the same skulls as in (A) and (B). The premaxillary suture of the mutant (D) shows remarkably weaker interdigitation (arrows) than that of the wild-type littermate (C).

(E and F) Lateral view of premaxillary sutures of the mutant mouse. The suture on the left side (F), i.e., ipsilateral to the direction of twisting of the snout, is straight and has smooth edges, as compared to the suture with serrated edges on the right side (E).

(G) Severe dental malocclusion in an *Il11ra* null mutant mouse. The maxillary (upper) teeth are in an abnormal posterior position.

jaw bones were devoid of *Il11ra* transcripts. These findings are in line with the observation from a microarray screen indicating that the expression of *IL11RA* was higher in nonfused than in fused sutures.[53] Thus, the expression analyses in craniofacial bones suggest that IL11 signaling does not affect the secretory function of osteoblasts but may affect osteoblast precursors and osteoclasts.

So far, defects in the regulation of proliferation and differentiation of the osteoblast precursors have been shown to contribute to craniosynostosis in the mouse models of the human syndromes caused by mutations in FGF receptors, *MSX2* (MIM 123101), *TWIST*, and *EFNB1*.[11] Our observations of premaxillary suture inactivation in the *Il11ra* null mutant mice are strikingly similar to those in mice with mutated *Fgfr*s,[33,54] suggesting that mutations in *IL11RA* have effects on suture maintenance similar to those in observed FGFRs. However, though not previously demonstrated, it is conceivable that failure of bone resorption may also lead to precocious synostosis of craniofacial bones. Active osteoclasts are present in the developing calvarial sutures of pre- and postnatal mice.[7] Our findings show that IL11 signaling is critical for the maintenance of suture patency. The available data suggest that the craniosynostosis phenotype seen in *IL11RA*-deficient humans and mice results from a failure to regulate bone remodeling, i.e., from an imbalance between bone apposition and resorption at the osteogenic fronts in the sutures. Given that the inactivation of *Il11ra* in mice appears to cause a cell-autonomous inhibition of osteoclast differentiation, it is possible that the synostoses observed in human patients and the null mutant mice result from a primary defect in bone resorption. Interestingly, ephrin signaling has recently been associated with communication between osteoclasts and osteoblasts, suggesting that defects in bone resorption may contribute to craniosynostosis caused by mutations in ephrins.[55]

The suggestion that the mutations in *IL11RA* caused impaired bone resorption is further supported by the delayed and ectopic tooth eruption in our patients. Localized resorption of the jaw bone by osteoclasts is a prerequisite for tooth eruption,[9] and indeed, increased expression of *Il11* has been associated with accelerated tooth eruption and increased bone resorption in *Mcp* (monocytic chemoattractant protein) null mutant mice.[56]

The association between *IL11RA* mutation and supernumerary teeth provides the first evidence that the IL11-RA-gp130pathway regulates patterning of any organ. The reported large incisors in family 2 may also present an effect of the *IL11RA* mutation on tooth development, but unfortunately we were not able to assess the dental phenotype in this family in detail. All the tooth types that are normally replaced once (namely incisors, canines, and premolars) were represented among the supernumerary teeth. They were, on average, 4 years delayed in development compared to the permanent teeth and localized on the lingual side of the jaw and occlusally to the permanent teeth. Thus, their developmental timing and location are strikingly similar to the supernumerary tooth phenotype associated with cleidocranial dysplasia, caused by haploinsufficiency of *RUNX2*.[15,16] It is possible to consider the supernumerary teeth in these syndromes as a representation of a third dentition,[15] and thus the mutations in *RUNX2* and *IL11RA* appear to unlock the capacity for multiple or continuous tooth replacements as seen in fish and reptiles. The absence of supernumerary teeth in the *Il11ra* and *Runx2* null mutants[57] is likely explained by an essential lack of capacity for tooth replacement in mice given that they only develop one set of teeth. The very similar phenotypes of supernumerary tooth formation resulting from cleidocranial dysplasia and *IL11RA* mutation, as well as the coexpression of *Runx2* and *Il11ra* in the craniofacial and dental mesenchyme,[57]

raise the possibility that the genes function in the same genetic pathway that potentially interacts with Wnt signaling.[13,14]

It is noteworthy that despite the similarity of the supernumerary tooth phenotype in the syndrome described here and in cleidocranial dysplasia, the bone phenotypes are directly opposite, because cleidocranial dysplasia features hypoplasia of cranial bones, with wide sutures and open fontanelles. In the case of *Runx2* there is evidence that the gene regulates tooth development independently of its effects on bone development.[57,58] Thus, it is possible that the effects of the *IL11RA* and *RUNX2* and their proposed interactions depend on the context.

In conclusion, we have shown that IL11 receptor signaling is needed to prevent premature craniofacial sutural fusion in man and mouse, to limit the formation of replacement teeth to the normal single set of secondary teeth in humans, and to allow normal tooth eruption. We suggest that the pathogenesis of delayed and ectopic tooth eruption involves impaired resorption and remodeling of bone due to the lack of IL11 signaling in the bone-resorbing osteoclasts and that this may also contribute to craniosynostosis. Furthermore, because IL11 is a negative regulator of suture closure, it is tempting to speculate that IL11 or other components of gp130 signaling could be applied therapeutically to prevent suture recurrence of craniosynostosis after surgery. The mutation in *IL11RA* is one of the few identified recessive causes of craniosynostosis in man, and it was identified because of the consanguinity in the affected families who displayed variable phenotypic features associated with craniosynostosis. Although *IL11RA* craniosynostosis syndrome appears to be infrequent, it is possible that mutations in other components of the IL11/gp130 signaling pathway may also contribute both to craniosynostosis and to supernumerary teeth.

Supplemental Data

Supplemental Data include four figures and one table and can be found with this article online at http://www.cell.com/AJHG.

Acknowledgments

We are grateful for Brendan Jenkins and Meegan Howlett in Melbourne, Australia, for collecting the mouse heads. We thank Lorraine Robb and Tracy Willson, Melbourne, for the plasmid containing human *IL11RA* cDNA and Syed Qasim Mehdi and Sayed Hajan Shah for providing Pakistani control DNA samples. The skilful technical help of Riikka Santalahti, Merja Mäkinen, Marjatta Kivekäs, Hanne Ahola, Maarit Hakkarainen, and Raija Savolainen is gratefully acknowledged. We thank Steve Twigg for help in curating the Oxford craniosynostosis samples and Clare Taylor for help with clinical review. We also thank Shanaz Pasha for help with collecting DNA and Louise Tee and Tim Forshew for genotyping the families. The project has been funded by the Academy of Finland (I.T.), Finnish Dental Society Apollonia (L.V., S.A.), the Sigrid Juselius Foundation (I.T.), HUCH EVO (P.N., S.A.), WellChild (N.V.M., E.R.M.), and Wellcome Trust (A.O.M.W; Programme Grant 078666).

Received: March 31, 2011
Revised: May 13, 2011
Accepted: May 25, 2011
Published online: July 7, 2011

Web Resources

The URLs for data presented herein are as follows:

1000 Genomes, http://www.1000genomes.org
dbSNP, http://www.ncbi.nlm.nih.gov/SNP
Eukaryotic Linear Motif (ELM), http://elm.eu.org
GenBank, http://www.ncbi.nlm.nih.gov
GenePaint, http://genepaint.org
NetCGlyc, http://www.cbs.dtu.dk/services/NetCGlyc
Online Mendelian Inheritance in Man (OMIM), http://www.omim.org
PolyPhen, http://genetics.bwh.harvard.edu/cgi-bin/pph
SIFT, http://sift.jcvi.org
SNPs3D, http://www.snps3d.org
STRING, http://string.embl.de

Accession Numbers

The submitted dbSNP numbers for the sequence variants reported in this paper are 342590391 (c.130G>A), 342590394 (c.871G>A), and 342590396 (c.1090_1104delGAGCAGGTAGCTGTG).

References

1. Morriss-Kay, G.M., and Wilkie, A.O.M. (2005). Growth of the normal skull vault and its alteration in craniosynostosis: insights from human genetics and experimental studies. J. Anat. *207*, 637–653.
2. Rice, D.P. (2005). Craniofacial anomalies: from development to molecular pathogenesis. Curr. Mol. Med. *5*, 699–722.
3. Thesleff, I., and Nieminen, P. (2005). Tooth induction. In Encyclopedia of Life Sciences. (Nature Publishing Group, Macmillan Publishers Ltd.) www.els.net.
4. Nieminen, P. (2009). Genetic basis of tooth agenesis. J. Exp. Zool. B Mol. Dev. Evol. *312B*, 320–342.
5. Haavikko, K. (1971). Hypodontia of permanent teeth. An orthopantomographic study. Suom. Hammaslaak. Toim. *67*, 219–225.
6. Zhu, J.F., Marcushamer, M., King, D.L., and Henry, R.J. (1996). Supernumerary and congenitally absent teeth: a literature review. J. Clin. Pediatr. Dent. *20*, 87–95.
7. Rice, D.P., Kim, H.J., and Thesleff, I. (1997). Detection of gelatinase B expression reveals osteoclastic bone resorption as a feature of early calvarial bone development. Bone *21*, 479–486.
8. Marks, S.C., Jr., and Schroeder, H.E. (1996). Tooth eruption: theories and facts. Anat. Rec. *245*, 374–393.
9. Wise, G.E., and King, G.J. (2008). Mechanisms of tooth eruption and orthodontic tooth movement. J. Dent. Res. *87*, 414–434.
10. Kreiborg, S. (2000). Postnatal growth and development of the craniofacial complex in premature craniosynostosis. In Craniosynostosis: Diagnosis, evaluation, and management, M.M. Cohen, Jr. and R.E. MacLean, eds. (New York: Oxford University Press), pp. 158–174.

11. Passos-Bueno, M.R., Serti Eacute, A.E., Jehee, F.S., Fanganiello, R., and Yeh, E. (2008). Genetics of craniosynostosis: genes, syndromes, mutations and genotype-phenotype correlations. Front Oral Biol. *12*, 107–143.
12. Ida, M., Nakamura, T., and Utsunomiya, J. (1981). Osteomatous changes and tooth abnormalities found in the jaw of patients with adenomatosis coli. Oral Surg. Oral Med. Oral Pathol. *52*, 2–11.
13. Järvinen, E., Salazar-Ciudad, I., Birchmeier, W., Taketo, M.M., Jernvall, J., and Thesleff, I. (2006). Continuous tooth generation in mouse is induced by activated epithelial Wnt/beta-catenin signaling. Proc. Natl. Acad. Sci. USA *103*, 18627–18632.
14. Wang, X.P., O'Connell, D.J., Lund, J.J., Saadi, I., Kuraguchi, M., Turbe-Doan, A., Cavallesco, R., Kim, H., Park, P.J., Harada, H., et al. (2009). Apc inhibition of Wnt signaling regulates supernumerary tooth formation during embryogenesis and throughout adulthood. Development *136*, 1939–1949.
15. Jensen, B.L., and Kreiborg, S. (1990). Development of the dentition in cleidocranial dysplasia. J. Oral Pathol. Med. *19*, 89–93.
16. Mundlos, S., Otto, F., Mundlos, C., Mulliken, J.B., Aylsworth, A.S., Albright, S., Lindhout, D., Cole, W.G., Henn, W., Knoll, J.H., et al. (1997). Mutations involving the transcription factor CBFA1 cause cleidocranial dysplasia. Cell *89*, 773–779.
17. Cohen, M.M., Jr., and MacLean, R.E. (2000). Craniosynostosis: Diagnosis, Evaluation, and Management. (New York: Oxford University Press).
18. Sobel, E., and Lange, K. (1996). Descent graphs in pedigree analysis: applications to haplotyping, location scores, and marker-sharing statistics. Am. J. Hum. Genet. *58*, 1323–1337.
19. Drmanac, R., Sparks, A.B., Callow, M.J., Halpern, A.L., Burns, N.L., Kermani, B.G., Carnevali, P., Nazarenko, I., Nilsen, G.B., Yeung, G., et al. (2010). Human genome sequencing using unchained base reads on self-assembling DNA nanoarrays. Science *327*, 78–81.
20. Ho, S.N., Hunt, H.D., Horton, R.M., Pullen, J.K., and Pease, L.R. (1989). Site-directed mutagenesis by overlap extension using the polymerase chain reaction. Gene *77*, 51–59.
21. Nandurkar, H.H., Robb, L., Tarlinton, D., Barnett, L., Köntgen, F., and Begley, C.G. (1997). Adult mice with targeted mutation of the interleukin-11 receptor (IL11Ra) display normal hematopoiesis. Blood *90*, 2148–2159.
22. Schleinkofer, K., Dingley, A., Tacken, I., Federwisch, M., Müller-Newen, G., Heinrich, P.C., Vusio, P., Jacques, Y., and Grötzinger, J. (2001). Identification of the domain in the human interleukin-11 receptor that mediates ligand binding. J. Mol. Biol. *306*, 263–274.
23. Yang, Y.C., and Yin, T. (1992). Interleukin-11 and its receptor. Biofactors *4*, 15–21.
24. Hilton, D.J., Hilton, A.A., Raicevic, A., Rakar, S., Harrison-Smith, M., Gough, N.M., Begley, C.G., Metcalf, D., Nicola, N.A., and Willson, T.A. (1994). Cloning of a murine IL-11 receptor alpha-chain; requirement for gp130 for high affinity binding and signal transduction. EMBO J. *13*, 4765–4775.
25. Yang, Y.C., and Yin, T. (1995). Interleukin (IL)-11—mediated signal transduction. Ann. N. Y. Acad. Sci. *762*, 31–40, discussion 40–41.
26. Dahmen, H., Horsten, U., Küster, A., Jacques, Y., Minvielle, S., Kerr, I.M., Ciliberto, G., Paonessa, G., Heinrich, P.C., and Müller-Newen, G. (1998). Activation of the signal transducer gp130 by interleukin-11 and interleukin-6 is mediated by similar molecular interactions. Biochem. J. *331*, 695–702.
27. Kiessling, S., Muller-Newen, G., Leeb, S.N., Hausmann, M., Rath, H.C., Strater, J., Spottl, T., Schlottmann, K., Grossmann, J., Montero-Julian, F.A., et al. (2004). Functional expression of the interleukin-11 receptor alpha-chain and evidence of anti-apoptotic effects in human colonic epithelial cells. J. Biol. Chem. *279*, 10304–10315.
28. Neuhaus, H., Bettenhausen, B., Bilinski, P., Simon-Chazottes, D., Guénet, J.L., and Gossler, A. (1994). Etl2, a novel putative type-I cytokine receptor expressed during mouse embryogenesis at high levels in skin and cells with skeletogenic potential. Dev. Biol. *166*, 531–542.
29. Robb, L., Li, R., Hartley, L., Nandurkar, H.H., Koentgen, F., and Begley, C.G. (1998). Infertility in female mice lacking the receptor for interleukin 11 is due to a defective uterine response to implantation. Nat. Med. *4*, 303–308.
30. Sims, N.A., Jenkins, B.J., Nakamura, A., Quinn, J.M., Li, R., Gillespie, M.T., Ernst, M., Robb, L., and Martin, T.J. (2005). Interleukin-11 receptor signaling is required for normal bone remodeling. J. Bone Miner. Res. *20*, 1093–1102.
31. Barton, V.A., Hall, M.A., Hudson, K.R., and Heath, J.K. (2000). Interleukin-11 signals through the formation of a hexameric receptor complex. J. Biol. Chem. *275*, 36197–36203.
32. Barton, V.A., Hudson, K.R., and Heath, J.K. (1999). Identification of three distinct receptor binding sites of murine interleukin-11. J. Biol. Chem. *274*, 5755–5761.
33. Twigg, S.R., Healy, C., Babbs, C., Sharpe, J.A., Wood, W.G., Sharpe, P.T., Morriss-Kay, G.M., and Wilkie, A.O.M. (2009). Skeletal analysis of the Fgfr3(P244R) mouse, a genetic model for the Muenke craniosynostosis syndrome. Dev. Dyn. *238*, 331–342.
34. Du, X., Everett, E.T., Wang, G., Lee, W.H., Yang, Z., and Williams, D.A. (1996). Murine interleukin-11 (IL-11) is expressed at high levels in the hippocampus and expression is developmentally regulated in the testis. J. Cell. Physiol. *168*, 362–372.
35. Jenkins, B.J., Roberts, A.W., Greenhill, C.J., Najdovska, M., Lundgren-May, T., Robb, L., Grail, D., and Ernst, M. (2007). Pathologic consequences of STAT3 hyperactivation by IL-6 and IL-11 during hematopoiesis and lymphopoiesis. Blood *109*, 2380–2388.
36. Ernst, M., Najdovska, M., Grail, D., Lundgren-May, T., Buchert, M., Tye, H., Matthews, V.B., Armes, J., Bhathal, P.S., Hughes, N.R., et al. (2008). STAT3 and STAT1 mediate IL-11-dependent and inflammation-associated gastric tumorigenesis in gp130 receptor mutant mice. J. Clin. Invest. *118*, 1727–1738.
37. Howlett, M., Menheniott, T.R., Judd, L.M., and Giraud, A.S. (2009). Cytokine signalling via gp130 in gastric cancer. Biochim. Biophys. Acta *1793*, 1623–1633.
38. Sims, N.A. (2009). gp130 signaling in bone cell biology: multiple roles revealed by analysis of genetically altered mice. Mol. Cell. Endocrinol. *310*, 30–39.
39. Rice, D.P., and Rice, R. (2008). Locate, condense, differentiate, grow and confront: developmental mechanisms controlling intramembranous bone and suture formation and function. Front Oral Biol. *12*, 22–40.
40. Blair, H.C., Robinson, L.J., and Zaidi, M. (2005). Osteoclast signalling pathways. Biochem. Biophys. Res. Commun. *328*, 728–738.

41. Proff, P., and Römer, P. (2009). The molecular mechanism behind bone remodelling: a review. Clin. Oral Investig. *13*, 355–362.

42. Suga, K., Saitoh, M., Fukushima, S., Takahashi, K., Nara, H., Yasuda, S., and Miyata, K. (2001). Interleukin-11 induces osteoblast differentiation and acts synergistically with bone morphogenetic protein-2 in C3H10T1/2 cells. J. Interferon Cytokine Res. *21*, 695–707.

43. Takeuchi, Y., Watanabe, S., Ishii, G., Takeda, S., Nakayama, K., Fukumoto, S., Kaneta, Y., Inoue, D., Matsumoto, T., Harigaya, K., and Fujita, T. (2002). Interleukin-11 as a stimulatory factor for bone formation prevents bone loss with advancing age in mice. J. Biol. Chem. *277*, 49011–49018.

44. Leon, E.R., Iwasaki, K., Komaki, M., Kojima, T., and Ishikawa, I. (2007). Osteogenic effect of interleukin-11 and synergism with ascorbic acid in human periodontal ligament cells. J. Periodontal Res. *42*, 527–535.

45. Suga, K., Saitoh, M., Kokubo, S., Fukushima, S., Kaku, S., Yasuda, S., and Miyata, K. (2003). Interleukin-11 acts synergistically with bone morphogenetic protein-2 to accelerate bone formation in a rat ectopic model. J. Interferon Cytokine Res. *23*, 203–207.

46. Suga, K., Saitoh, M., Kokubo, S., Nozaki, K., Fukushima, S., Yasuda, S., Sasamata, M., and Miyata, K. (2004). Synergism between interleukin-11 and bone morphogenetic protein-2 in the healing of segmental bone defects in a rabbit model. J. Interferon Cytokine Res. *24*, 343–349.

47. Kido, S., Kuriwaka-Kido, R., Imamura, T., Ito, Y., Inoue, D., and Matsumoto, T. (2009). Mechanical stress induces Interleukin-11 expression to stimulate osteoblast differentiation. Bone *45*, 1125–1132.

48. Romas, E., Udagawa, N., Zhou, H., Tamura, T., Saito, M., Taga, T., Hilton, D.J., Suda, T., Ng, K.W., and Martin, T.J. (1996). The role of gp130-mediated signals in osteoclast development: regulation of interleukin 11 production by osteoblasts and distribution of its receptor in bone marrow cultures. J. Exp. Med. *183*, 2581–2591.

49. Hill, P.A., Tumber, A., Papaioannou, S., and Meikle, M.C. (1998). The cellular actions of interleukin-11 on bone resorption in vitro. Endocrinology *139*, 1564–1572.

50. Horwood, N.J., Elliott, J., Martin, T.J., and Gillespie, M.T. (1998). Osteotropic agents regulate the expression of osteoclast differentiation factor and osteoprotegerin in osteoblastic stromal cells. Endocrinology *139*, 4743–4746.

51. Ahlen, J., Andersson, S., Mukohyama, H., Roth, C., Bäckman, A., Conaway, H.H., and Lerner, U.H. (2002). Characterization of the bone-resorptive effect of interleukin-11 in cultured mouse calvarial bones. Bone *31*, 242–251.

52. Kudo, O., Sabokbar, A., Pocock, A., Itonaga, I., Fujikawa, Y., and Athanasou, N.A. (2003). Interleukin-6 and interleukin-11 support human osteoclast formation by a RANKL-independent mechanism. Bone *32*, 1–7.

53. Coussens, A.K., Wilkinson, C.R., Hughes, I.P., Morris, C.P., van Daal, A., Anderson, P.J., and Powell, B.C. (2007). Unravelling the molecular control of calvarial suture fusion in children with craniosynostosis. BMC Genomics *8*, 458.

54. Hajihosseini, M.K., Wilson, S., De Moerlooze, L., and Dickson, C. (2001). A splicing switch and gain-of-function mutation in FgfR2-IIIc hemizygotes causes Apert/Pfeiffer-syndrome-like phenotypes. Proc. Natl. Acad. Sci. USA *98*, 3855–3860.

55. Martin, T., Gooi, J.H., and Sims, N.A. (2009). Molecular mechanisms in coupling of bone formation to resorption. Crit. Rev. Eukaryot. Gene Expr. *19*, 73–88.

56. Graves, D.T., Alsulaimani, F., Ding, Y., and Marks, S.C., Jr. (2002). Developmentally regulated monocyte recruitment and bone resorption are modulated by functional deletion of the monocytic chemoattractant protein-1 gene. Bone *31*, 282–287.

57. D'Souza, R.N., Åberg, T., Gaikwad, J., Cavender, A., Owen, M., Karsenty, G., and Thesleff, I. (1999). Cbfa1 is required for epithelial-mesenchymal interactions regulating tooth development in mice. Development *126*, 2911–2920.

58. Åberg, T., Wang, X.P., Kim, J.H., Yamashiro, T., Bei, M., Rice, R., Ryoo, H.M., and Thesleff, I. (2004). Runx2 mediates FGF signaling from epithelium to mesenchyme during tooth morphogenesis. Dev. Biol. *270*, 76–93.